# Effects of the Crystalline Structure of Purple Membrane on the Kinetics and Energetics of the Bacteriorhodopsin Photocycle†

György Váró‡ and Janos K. Lanyi*
*Department of Physiology and Biophysics, University of California, Irvine, California 92717*
*Received March 7, 1991; Revised Manuscript Received April 22, 1991*

ABSTRACT: Time-resolved difference spectra were measured for Triton X-100 solubilized bacteriorhodopsin monomers between 100 ns and 100 ms after photoexcitation. The results are consistent with the general scheme K ↔ L ↔ $M_1$ → $M_2$ ↔ N ↔ O → BR proposed previously for purple membranes [Váró, G., & Lanyi, J. K. (1990) *Biochemistry 29*, 2241–2250]. The rate constants which involve proton release or uptake, i.e., $k_{LM1}$, $k_{NO}$, and $k_{ON}$, were significantly higher in the monomeric protein than in purple membrane; the other steps were less affected. Analysis of the temperature dependencies of the rate constants between 5 and 30 °C yielded the enthalpies and entropies of activation for all steps except the two absent back-reactions. Comparison of these with data for purple membranes [Váró, G., & Lanyi, J. K. (1991) *Biochemistry 30*, 5016–5022] shows that the crystalline structure affects the energetics of the photocycle. In bacteriorhodopsin immobilized by the lattice of the purple membrane, the entropy changes leading to all transition states are more positive. Thus, the forward reactions proceed with less conformational hindrance. However, the thermal (enthalpic) barriers are higher. These effects are particularly pronounced for the $M_1$ → $M_2$ and O → BR reactions. Large changes of the enthalpy and entropy levels of intermediates in the $M_2$ → BR reaction segment, but not in the K → $M_1$ segment, upon solubilization of the protein are consistent with our earlier proposal that major protein conformational changes occur in the photocycle and they begin with the $M_1$ → $M_2$ reaction.

A number of recent reports have suggested that the photocycle associated with light-driven proton transport in the retinal protein bacteriorhodopsin (BR) is a single linear reaction sequence of the spectroscopically distinguishable intermediates J, K, L, M, N, and O, which contain several reversible reactions of significant rates (Chernavskii et al., 1989; Otto et al., 1989; Váró & Lanyi, 1990, 1991a,b,c; Ames & Mathies, 1990; Gerwert et al., 1990). Light causes all-trans to 13-cis isomerization of the retinal; during the photocycle, the retinal is thermally reisomerized, and the initial chromophore state recovers within tens of milliseconds while a proton is translocated from the cytoplasmic to the extracellular side. The initial consequence of the retinal isomerization is to lower the p$K_a$ of the retinal Schiff base, i.e., to labilize its proton. Vectorial movement of protons across the membrane is ensured by the fact that in the L to M reaction the proton is transferred from the Schiff base to D85 (Braiman et al., 1988; Butt et al., 1989; Tittor et al., 1989; Gerwert et al., 1990) which has access to the extracellular side (Henderson et al., 1990), while in the M to N reaction the Schiff base regains a proton from D96 (Gerwert et al., 1989, 1990; Butt et al., 1989; Tittor et al., 1989; Otto et al., 1989) which has access to the cytoplasmic side (Henderson et al., 1990). Recently the M intermediate was kinetically and spectroscopically resolved into two sequential substates, $M_1$ and $M_2$ (Váró & Lanyi, 1991a). The $M_1$ to $M_2$ reaction is virtually irreversible and results in considerable decrease of the entropy of the system [by about 300 J/(mol·K)], suggesting a large-scale protein conformational change (Ort & Parson, 1979; Váró & Lanyi, 1991b). In this step, part of the free energy is used to generate a proton gradient, and the rest is transferred from the chromophore to the protein. In our interpretation of the thermodynamic data, the $M_1$ → $M_2$ reaction has three essential functions: (1) it raises the p$K_a$ of the Schiff base so as to make it a proton acceptor in the next step of the photocycle; (2) it changes access of the Schiff base from D85 and the extracellular side to D96 and the cytoplasmic side; and (3) it is the coupling step which provides a large free energy barrier against backpressure from the protonmotive force created (Váró & Lanyi, 1991b).

BR is a small integral membrane protein located in trimers which are arranged in extended two-dimensional hexagonal arrays (purple membrane) in the cytoplasmic membrane of halobacterial cells (Blaurock & Stoeckenius, 1971; Henderson & Unwin, 1975). The crystalline lattice confers remarkable resistance to the protein against denaturation by heat as well as by high and low pH [e.g., see Brouillette et al. (1987)]. This is unlikely to be its physiological rationale, however. In considering the importance of the lattice, we note, on the one hand, that (1) the photocycle is not greatly changed when BR is converted to monomers (Dencher et al., 1983; Fukuda et al., 1990; Milder et al., 1991; Váró & Lanyi, 1991a) and (2) monomeric BR retains proton transport activity when incorporated into lipid bilayers (Dencher & Heyn, 1979; Bamberg et al., 1981). We would expect, on the other hand, that large-scale conformational changes (Ormos, 1991; Koch et al., 1991), which appear to underlie the $M_1$ → $M_2$ reaction and the subsequent pathway leading back to BR, would be sensitive to removal of the considerable motional constraints present in the crystalline lattice (Cherry et al., 1977; Czégé et al., 1982). In this study, we describe some thermodynamic parameters of the photoreaction of monomeric BR and compare it to previous results with purple membranes (Váró & Lanyi, 1991b). In interpreting the data, we have paid particular attention to the activation enthalpies and entropies associated with the calculated microscopic rate constants, and their physical meanings, in the context of the energetics of this proton pump. As expected, in the lattice but not in monomeric

† This work was supported by grants from the National Institutes of Health (GM 29498) and the National Aeronautics and Space Administration (NAGW-212).
* To whom correspondence should be addressed.
‡ Permanent address: Biological Research Center of the Hungarian Academy of Sciences, Szeged, Hungary.

0006-2960/91/0430-7165$02.50/0 

BR, the thermal barriers dominate over the entropic factors. The greatest effects of the crystalline lattice are on those photocycle steps where conformational changes are thought to occur.

## Materials and Methods

Purple membranes were isolated from *Halobacterium halobium* S9 as described before (Oesterhelt & Stoeckenius, 1974). All the measurements were in 100 mM NaCl/50 mM phosphate buffer, pH 7.0. Solubilization was with 2% Triton X-100 in the absence of salt. The circular dichroism spectrum in the visible, determined with a Jasco Model J-720 spectrometer, indicated that after incubation for 2 days at room temperature in the dark and centrifugation to remove a small amount of unsolubilized material the BR was entirely in the monomeric state. After solubilization, NaCl and buffer were added. All samples were light-adapted before the measurements.

Time-resolved difference spectra were obtained with a gated optical multichannel analyzer after subnanosecond laser photoexcitation at 580 nm as described (Zimányi et al., 1989). As before, magic-angle polarization was used to avoid effects from chromophore reorientation. The laser repetition rate was 0.5–4 Hz depending on the longest relaxation time in the samples. Averaging was over 200–1000 traces. Temperature was controlled within ±0.1 °C. From the same data, spectra of the BR without flash excitation were also obtained; these showed that the sample did not change optically during the flash regimes.

## Results

*Solubilization of Bacteriorhodopsin.* The preparation of BR monomers was as described by Dencher and Heyn (1978). Purple membrane was solubilized by 2-days incubation at room temperature with 2% Triton X-100 in the absence of salt. After this time, the absorption maximum of the sample shifted from 568 to 552 nm, and only a negligible fraction was sedimentable at 15000*g* over 20 min. In the CD spectrum of the supernatant after centrifugation (not shown), the characteristic bi-lobe structure was lost. The shapes and measured amplitudes agreed quantitatively with CD spectra of purple membrane and Triton X-100 solubilized BR reported before under similar conditions [e.g., see Becher and Ebrey (1976)]. The CD changes thus indicated that exciton interaction between chromophores within the BR trimers (Heyn et al., 1975; Bauer et al., 1976) was disrupted. By all of these criteria, therefore, the detergent-treated protein was in the monomeric state.

*Measurement of Difference Spectra and Their Analysis.* Time-resolved difference spectra were determined after photoexcitation with a <1-ns laser pulse as before (Vârô & Lanyi, 1991a), at 5, 10, 15, 20, 25, and 30 °C. Representative spectra are shown for three of these temperatures in Figure 1A–F. The data show that the shapes of the spectra are not greatly changed by varying the temperature but the time course of their development is accelerated at the higher temperatures. It is known that light-adapted detergent-solubilized BR contains some 13-cis chromophore (Casadio & Stoeckenius, 1980; Casadio et al., 1980) but because its amount is low and the difference spectra from the 13-cis photocycle have much smaller amplitudes than those from the all-trans cycle (Hofrichter et al., 1989) we considered it a reasonable approximation to neglect its contribution.

The measured time-resolved difference spectra for solubilized BR, such as in Figure 1, were used to calculate the time-dependent concentrations of the photocycle intermediates. The method and the assumptions used in these calculations were previously described (Vârô & Lanyi, 1991a,c). Briefly, we first derived absorption spectra for the intermediates from a subset of the difference spectra. This was done by an iterative multiparameter search until all of the spectra obeyed, simultaneously, the following criteria: no negative absorption, single peaks, and agreement with predictions from retinal excited states and reported ethylenic stretch frequencies. We had reported such a set of spectra for Triton X-100 solubilized BR already (Vârô & Lanyi, 1991a), which included spectra for K, L, $M_1$, $M_2$, N, and O; unlike in purple membranes, however, the maxima for $M_1$ and $M_2$ were distinguished by a small wavelength shift. The time-dependent concentrations of the intermediates were then calculated with the assumption that all measured difference spectra were weighted sums of the component difference spectra defined by the spectra of these intermediates.

Figure 2A–C shows the calculated time-resolved concentrations at 10, 20, and 30 °C (points). The photocycle scheme we had proposed earlier for purple membranes, BR $\xrightarrow{h\nu}$ K $\leftrightarrow$ L $\leftrightarrow$ $M_1$ $\rightarrow$ $M_2$ $\leftrightarrow$ N $\leftrightarrow$ O $\rightarrow$ BR plus N $\rightarrow$ BR [e.g., Figure 5B in Vârô and Lanyi (1990b)], fits these points reasonably well (lines), provided that the N $\rightarrow$ BR shunt is assigned zero rate. It should be noted that even though the net absorption increases in the red region are small during the second half of the photocycle (Figure 1, panels B, D, and F), this is not because the transient accumulation of O is less but because of an apparent blue-shift in the spectrum of this species (Vârô & Lanyi, 1991a). At 20 °C, all but three of the calculated rate constants were within factors of 2–3 of those for purple membranes. The exceptions were $k_{LM1}$, which was 10 times greater in the solubilized sample [faster L $\leftrightarrow$ M equilibration in the presence of detergent was noted also by Milder et al. (1991)], and $k_{NO}$ and $k_{ON}$, which were 30 and 40 times greater, respectively [data in the legend to Figure 2 in this paper and in the legend to Figure 3 in Vârô and Lanyi (1991a)]. Interestingly, these three are the only steps in the photocycle in which protons are released or taken up by the protein. It is not clear why these reactions should be accelerated when the purple membrane lattice is disrupted. Fukuda et al. (1990) found that partial removal of phospholipid from purple membrane slowed down N decay, a result expected from less surface charge in these samples and therefore higher surface pH. The extensive removal of lipid from our samples upon solubilization should have also caused such an effect, but a higher surface pH does not account for the observed increase in the rates. A possible explanation might be that proton exchange between the interior and the aqueous phase is faster because of greater motional freedom of side chains in the detergent-solubilized protein.

It is instructive to consider how the data and model for solubilized BR in Figure 2 illustrate the consequences of having a set of reversible reactions in each of the two halves of the photocycle. Thus, first the concentrations of K, L, and $M_1$ become fixed in an equilibrium mixture with constant proportions and decay together with the time constant of the irreversible $M_1$ $\rightarrow$ $M_2$ reaction. Then, the concentrations of $M_2$, N, and O become fixed in a second equilibrium mixture with constant proportions and decay together with the time constant of the irreversible O $\rightarrow$ BR reaction. Although the underlying reasons for this behavior are present also in purple membrane, the multiple equilibria were not as evident in that system because $M_1$ and $M_2$ had the same spectra and the N $\rightarrow$ BR reaction prevented the development of the second kinetic equilibrium. As expected, the overall effect of increasing temperature is to increase the rate of each transition. Inter-

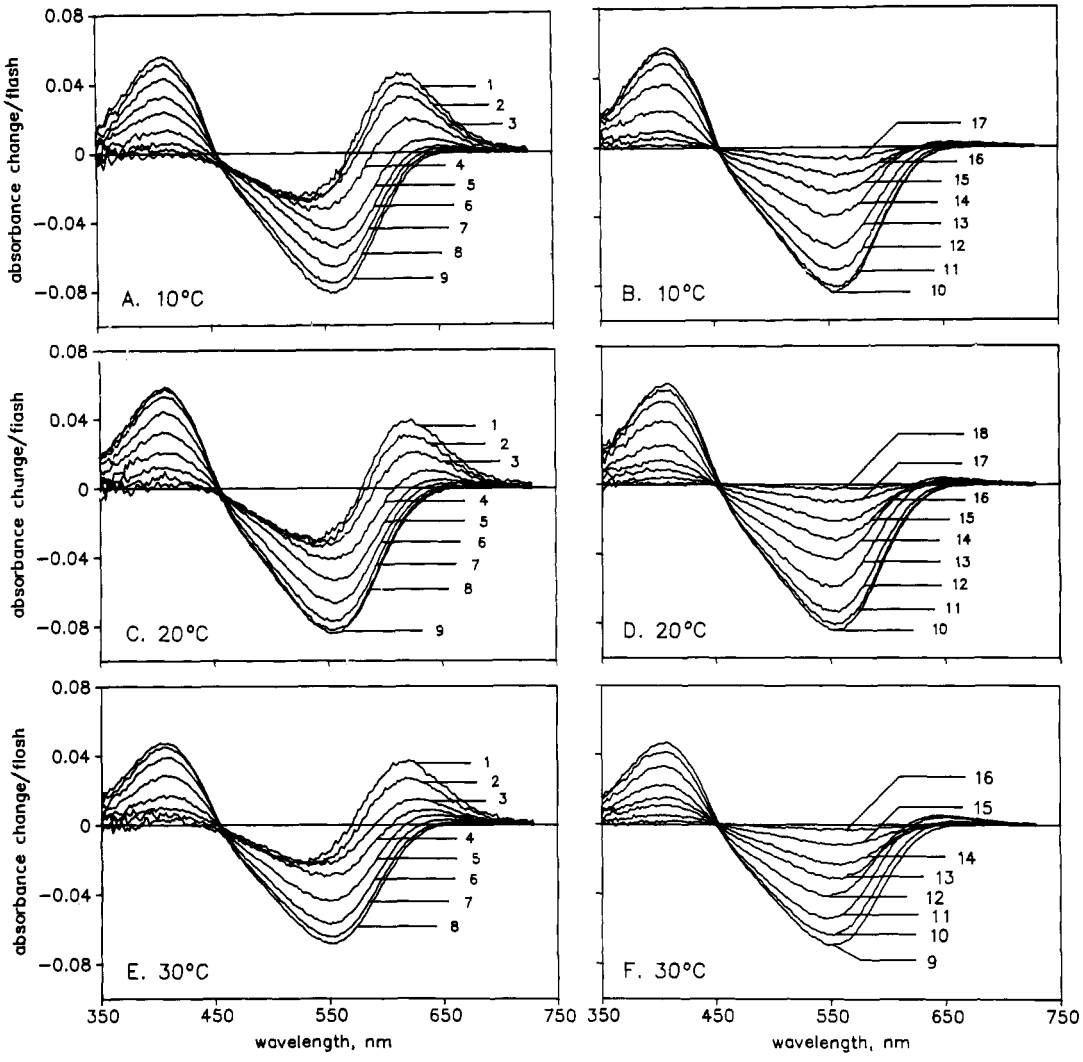


FIGURE 1: Measured difference spectra at 10 °C (A and B), 20 °C (C and D), and 30 °C (E and F). Delay times between the flash and the measurements are indicated by numbers from 1 through 18 which refer to 100 ns, 250 ns, 600 ns, 1.5 μs, 4 μs, 10 μs, 25 μs, 60 μs, 150 μs, 400 μs, 1 ms, 2.5 ms, 6 ms, 15 ms, 40 ms, 100, and 250 ms. Conditions: BR (solubilized with 2% Triton X-100) at 40 nmol/mL, in 100 mM NaCl/50 mM phosphate, pH 7.0, at the indicated temperatures.

estingly, the steep temperature dependency of the accumulation of O in purple membrane (Lozier et al., 1978; Li et al., 1984; Váró & Lanyi, 1991b) is not obtained in the solubilized BR.

*Activation Parameters in the Photocycle of Solubilized Bacteriorhodopsin.* According to transition-state theory, the rate of a reaction is proportional to the concentration of the state at the highest point on the free energy surface between the reactant(s) and product(s). The concentration of this state depends on the free energy increment over the initial state (resolved into enthalpy and entropy components), while the proportionality factor contains the frequency of the vibration of the chemical bonds which undergo the reaction. The rate of a first-order reaction is thus described by the equation:

$$\ln k_i = \ln \frac{kT}{h} + \frac{\Delta S_i^*}{R} - \frac{\Delta H_i^*}{RT} \qquad (1)$$

where $k_i$ is the rate constant of reaction $i$, $k$ is the Boltzmann constant, $T$ is the absolute temperature, $h$ is Planck's constant, $R$ is the gas constant, and $\Delta H_i^*$ and $\Delta S_i^*$ are the enthalpy and entropy changes required to reach the $i$th transition state.

Equation 1 relates the enthalpy, entropy, and free energy of activation to the rate constant and the temperature. The temperature dependencies of the rate constants which produced the fits in Figure 2 thus permit evaluation of the activation parameters of each of the reactions. As shown in Figure 3, the data fit eq 1 well. It should be noted that in such calculations the $\Delta H_i^*$s are determined largely by the slopes, and the $\Delta S_i^*$s are determined largely by the intercepts.

Since the enthalpy of activation, $\Delta H_i^*$, is the enthalpy increase from the initial to the transition state, i.e., a thermal barrier, for reactions catalyzed by proteins it reflects breaking hydrogen bonds, stretching or twisting covalent bonds, and overcoming internal attractive or repulsive Coulombic effects, unfavorable induced dipole moments, etc. Table I lists the calculated enthalpies of activation for the reactions in the BR photocycle, both in purple membrane [from data in Váró and Lanyi (1991b)] and in Triton X-100 micelles (from Figure 3 in this work). It is evident that solubilization changes the enthalpic description of the photocycle. Strikingly, in the monomeric BR, the barriers to many of the reactions are lower, most prominently for those of the unidirectional $M_1 \rightarrow M_2$ and $O \rightarrow BR$ transitions.

Interpreting these effects requires that any changes in the enthalpies of the intermediate states be distinguished from those of the transition states. In general, a change in a barrier height can mean either that the reaction proceeds via the same transition state but the enthalpy of the initial state has been changed or that the enthalpy of the initial state is the same but the reaction proceeds via a different transition state. Since the difference in the enthalpies of two successive stable states

Table I: Thermodynamic Parameters of the Photocycle of Bacteriorhodopsin in Purple Membrane and in Triton X-100 Micelles[a]

| | purple membrane | | | solubilized BR | | |
|---|---|---|---|---|---|---|
| reaction | $\Delta H^*$ | $\Delta S^*$ | $\Delta G^*$ | $\Delta H^*$ | $\Delta S^*$ | $\Delta G^*$ |
| K → L | 41 ± 1 | 10 ± 4 | 38 ± 2 | 35 ± 5 | −23 ± 5 | 42 ± 7 |
| L → K | 66 ± 6 | 73 ± 22 | 44 ± 9 | 55 ± 4 | 40 ± 13 | 43 ± 6 |
| L → $M_1$ | 70 ± 2 | 81 ± 8 | 46 ± 3 | 40 ± 5 | −18 ± 16 | 45 ± 9 |
| $M_1$ → L | 56 ± 2 | 40 ± 7 | 44 ± 3 | 30 ± 4 | −56 ± 13 | 47 ± 6 |
| $M_1$ → $M_2$ | 48 ± 1 | 0 ± 4 | 48 ± 2 | 28 ± 1 | −90 ± 3 | 55 ± 2 |
| $M_2$ → N | 67 ± 3 | 35 ± 10 | 57 ± 4 | 60 ± 2 | −1 ± 8 | 60 ± 5 |
| N → $M_2$ | 37 ± 5 | −73 ± 10 | 59 ± 6 | 55 ± 6 | 44 ± 13 | 61 ± 9 |
| N → O | 63 ± 2 | 17 ± 6 | 58 ± 3 | 45 ± 3 | −31 ± 10 | 54 ± 6 |
| O → N | 9 ± 1 | −162 ± 2 | 59 ± 3 | 22 ± 1 | −102 ± 4 | 53 ± 2 |
| N → BR | 67 ± 2 | 163 ± 8 | 58 ± 2 | | | |
| O → BR | 57 ± 2 | −8 ± 5 | 59 ± 2 | 25 ± 2 | −134 ± 8 | 65 ± 5 |

[a] Enthalpies and free energies of activation, $\Delta H^*$ and $\Delta G^*$, expressed in kilojoules per mole; entropy of activation, $\Delta S^*$, expressed in joules per mole per degrees kelvin. $\Delta G^*$ calculated for 20 °C. Data for purple membrane from Vārō and Lanyi (1991b). Data for Triton X-100 solubilized monomeric BR calculated from fitting eq 1 to the results in Figure 3. The N → BR step (Vārō et al., 1990) seems to be absent in monomeric BR.

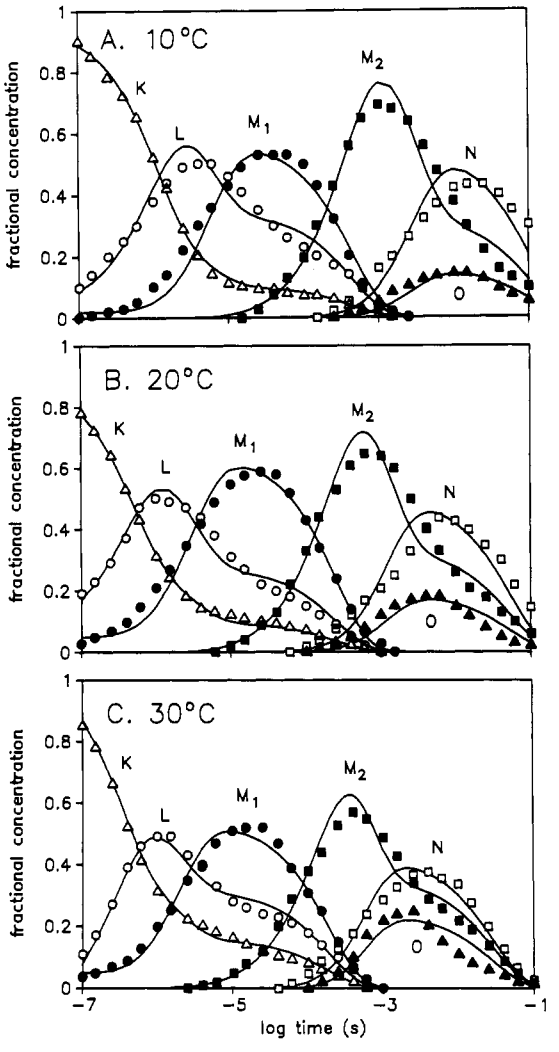


FIGURE 2: Calculated time-dependent concentrations of the photocycle intermediates at 10 (A), 20 (B), and 30 °C (C) and best fits of the kinetic model in the text. (△) K; (○) L; (●) $M_1$; (■) $M_2$; (□) N; (▲) O. Rate constants used (the three numbers represent values for 10, 20, and 30 °C in sequence, in $s^{-1}$): $k_{KL}$ = 6.7 × $10^5$, 1.43 × $10^6$, 2.0 × $10^6$; $k_{LK}$ = 2.0 × $10^5$, 5.0 × $10^5$, 9.09 × $10^5$; $k_{LM1}$ = 1.43 × $10^5$, 3.03 × $10^5$, 4.35 × $10^5$; $k_{M1L}$ = 8.33 × $10^4$, 1.25 × $10^5$, 2.5 × $10^5$; $k_{M1M2}$ = 4.0 × $10^3$, 6.25 × $10^3$, 1.0 × $10^4$; $k_{M2N}$ = 250, 625, 1538; $k_{NM2}$ = 143, 400, 1250; $k_{NO}$ = 3.7 × $10^3$, 6.25 × $10^3$, 1.43 × $10^4$; $k_{ON}$ = 1.25 × $10^4$, 1.67 × $10^4$, 2.5 × $10^4$; and $k_{OBR}$ = 63, 100, 143.

is equal to the difference between the reverse and the forward enthalpies of activation, the levels could be evaluated for those intermediates which participate in reversible reactions, i.e., K, L, $M_1$ and $M_2$, N, and O, as shown in Figure 4 (where the

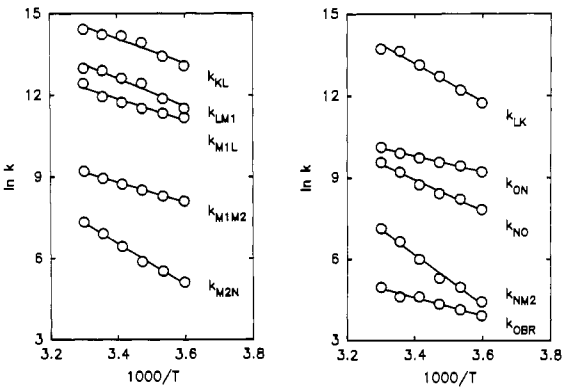


FIGURE 3: Eyring plot of the relationship of the calculated microscopic rate constants in Figure 2 to temperature. The lines are nonlinear least-squares fits to eq 1.

reference state is BR). The enthalpy levels of K, L, and $M_1$ relative to each other are clearly similar in the solubilized sample and purple membranes. This suggests that the observed lowering of the barriers in this reaction segment is caused by transition-state enthalpies which are altered relative to BR rather than by altered enthalpies of the intermediates. The situation is more complex after $M_2$. A steep rise in the enthalpies from $M_2$ to O is not seen in the solubilized sample (compare Figure 4A and Figure B). Here the apparent changes in the barrier heights are as likely to be caused by changed enthalpies of the intermediates as by different transition-state enthalpies; the data suggest that both had occurred. Because the enthalpy level of N is higher, the N → O reaction is less endothermic than in purple membranes (compare Figure 4A and Figure B); this is what causes the accumulation of O to be less temperature-dependent, as mentioned above. The relative enthalpy levels of $M_1$ and $M_2$ are not given by the data because the $M_2$ → $M_1$ back-reaction is not fast enough to be measured. This parameter is shown in Figure 4B as a reasonable estimate only: if the enthalpy of $M_2$ were not raised to within at least 25 kJ/mol of the value we show, the enthalpy of activation for the BR to O back-reaction would become negative and contradict the concept of the transition state for an elementary process. With this assumption, the $M_2$ to $M_1$ back-reaction in monomeric BR has an apparently greatly lowered barrier as compared to the lattice-immobilized BR. We conclude from these arguments that solubilization lowers the enthalpy levels for the transition states throughout, changes the enthalpy levels of the intermediates in the second half of the photocycle, and strongly decreases the thermal barrier to the $M_2$ to $M_1$ back-reaction.

Solubilization changes the entropic description of the pho-

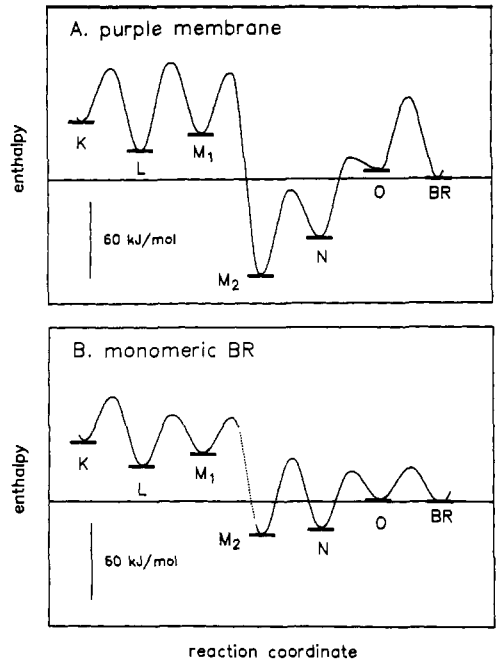


FIGURE 4: Enthalpy levels and barriers for the photocycle in purple membranes (A) and monomeric BR (B). For purple membrane, the activation enthalpies are from Váró and Lanyi (1991b); for monomeric BR, from Figure 3. The levels of the intermediates are given by the differences between activation enthalpies of the reverse and forward reactions. The level of K is assumed to be about 49 kJ/mol above that of BR (Birge et al., 1991). Since the rates of the $M_2 \rightarrow M_1$ and BR → O back-reactions could not be measured, the relative enthalpy levels of the $K \rightarrow M_1$ and $M_2 \rightarrow O$ reaction segments to each other and to that of BR are not determined. For purple membrane (A), they were estimated from independent calorimetric data (Ort & Parson, 1979), but for solubilized BR such data are not available. The enthalpy level of the $M_2$ to O segment in B was therefore adjusted so as to obtain a positive barrier between O and BR. This criterion would allow the enthalpy of $M_2$ to be higher, but not more than 25 kJ/mol lower, than shown. To indicate that this is an estimation, the activation enthalpy of the $M_2$ to $M_1$ back-reaction is drawn with a dotted line.

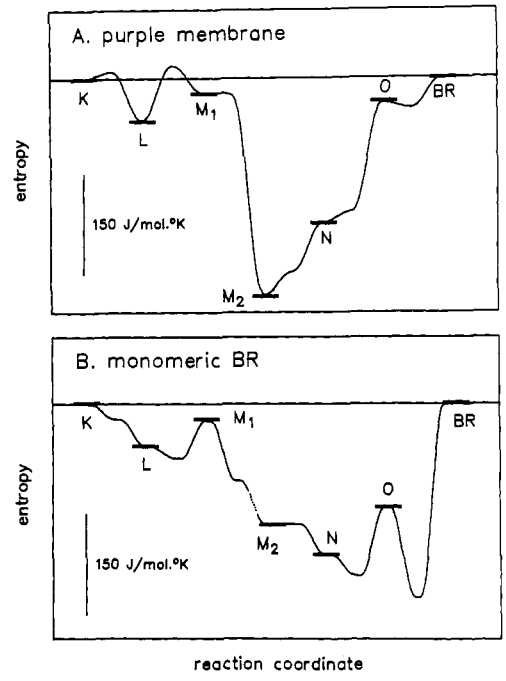


FIGURE 5: Entropy levels of intermediates and transition states for the photocycle in purple membranes (A) and monomeric BR (B). For purple membrane, the data are from Váró and Lanyi (1991b); for monomeric BR, from Figure 3. As with the enthalpies, the relative entropy levels of the $K \rightarrow M_1$ and $M_2 \rightarrow O$ reaction segments are not defined. They are drawn with the assumption of zero entropy difference between K and BR, and an entropy difference between $M_1$ and $M_2$ calculated from the enthalpy levels in Figure 4B in the same way as for purple membranes (Váró & Lanyi, 1991b). Because of this uncertainty, the activation entropy of the $M_2$ to $M_1$ back-reaction is drawn with a dotted line.

tocycle even more significantly. As with enthalpies, the entropy of activation represents the difference in the entropy of the transition state and the initial state in each reaction. A transition state with high entropy of activation represents a conformation which is more random compared to the initial state, while one with low entropy of activation is a statistically less probable, more ordered conformation. As shown in Table I, in solubilized BR, the entropies of the transition states are strongly lowered for nearly all reactions. Figure 5A,B compares the entropy levels for intermediates of purple membrane and solubilized BR. In the first half of the photocycle, the relative entropy levels are unchanged; in the second half, the pattern of the entropy levels of the intermediates is considerably altered. Thus, as with the enthalpies, it is after $M_1$ that the most striking differences caused by solubilization are observed. The entropy decrease in the $M_1 \rightarrow M_2$ reaction is much smaller and recovers not in two steps over the $M_2$ to O segment but mainly in the O → BR step. We had suggested (Váró & Lanyi, 1991b) that these entropy changes represent protein conformational changes and that when the protein is immobilized in the purple membrane the largest part of the conformational recovery is during the N → O reaction. Koch et al. (1991) made a similar conclusion on the basis of the pH dependency of time-resolved diffraction changes. In contrast, for nomomeric BR, the conformational recovery does not happen until after O. Indeed, here the greatest entropic (i.e., conformational) impediment in the photocycle is at the O → BR reaction (Figure 5B). It may be for this reason that in these samples recovery of BR is necessarily via the O state while in purple membranes O was not an obligatory member of the photocycle (Váró et al., 1990).

## Discussion

It appears from the results that there are consistent differences between the energetics of the BR photocycle in the crystalline lattice and in the detergent-solubilized monomeric state. The lowered activation enthalpies observed throughout indicate that in the monomers the transition states, particularly in the $M_1 \rightarrow M_2$ reaction, can be characterized as structurally *relaxed*, i.e., at a lower thermal energy. The lowered entropies of the transition states in the monomers indicate, on the other hand, that reaching the conformations required for all of the forward reactions is by processes which lead to increased order. This would be expected if the enzyme assumed a much larger number of isoenergetic configurational/conformational states in the detergent micelles than in the crystalline lattice, so that attaining the same transition states as in the purple membrane lead to reduction in the numbers of possible conformations. The results suggest, therefore, that the conformational restrictions on the transition states are greater than on the photocycle intermediates. We note, however, that entropies of protein reactions will be influenced also by any changes in the amount of structured water (Sturtevant, 1977; Baldwin, 1986; Murphy et al., 1990). For the glucose carrier in erythrocytes, for example, the occluded state during the translocation had a higher rather than lower entropy (Walmsley & Lowe, 1987); this was attributed to the transient dehydration of the substrate and/or the binding site. Presumably, here the entropy gain upon the disordering of water was greater than the probable entropy loss due to conforma-

tional rearrangement of the protein. We have argued (Vârô & Lanyi, 1991b) that in purple membranes such effects of water structure are minimal.

With the results in this report, we now have thermodynamic data for the BR photocycle both when this protein is located in the lattice of the purple membrane and when it is in the monomeric form. It is evident from the data that the rigidly fixed structure of the purple membrane *limits the protein to a relatively small number of conformations so that access to the transition states for passing through the photocycle reactions will be entropically favored.* The consistently higher activation enthalpies relative to monomeric BR indicate that this is accomplished at the expense of unfavorable bond strains and torsions, Coulombic interactions, etc. in at least some of the intermediates and transition states. We have suggested on other grounds (Vârô & Lanyi, 1991b) that in the K to $M_1$ segment of the photocycle the excess free energy remains at the chromophore (i.e., in the vicinity of the retinal and the residues with which it directly interacts) while in the $M_2$ to BR segment the excess free energy is mainly a property of the protein. Thus, the thermodynamics in the first half of the photocycle should reflect the reactions of the chromophore but in the second half conformational changes of protein. Consistent with this, we now find that the enthalpy and entropy levels of K, L, and $M_1$ are virtually unaffected by the crystalline lattice while those of $M_2$, N, and O are strongly changed (Figures 4 and 5). Thus, the results provide further support to the suggestion that major protein conformational changes occur in the photocycle beginning with the $M_1$ to $M_2$ step.

In purple membranes, the $M_1$ to $M_2$ reaction appears to be accompanied by a larger enthalpy and entropy decrease than in monomeric BR. The conformational change which accompanies the switch event in the pump is therefore more extensive when the protein is in the lattice: the lattice seems to ensure that the protein will assume a more highly ordered $M_2$ state. Consistent with this, the conspicuous changes in the activation parameters for the $M_1 \rightarrow M_2$ transition (Table I) indicate that the crystalline state presents a higher thermal barrier but much less entropic hindrance to the reaction than the monomeric state.

As often the case in proteins, the opposing entropy and enthalpy terms compensate one another so that the free energies (Table I), and therefore the reaction rates, are not greatly affected. In BR monomers just as in purple membranes, the net free energy changes in the reversible reactions (i.e., all reactions but $M_1 \rightarrow M_2$ and $O \rightarrow BR$) are near zero (Table I). As Albery and Knowles (1976) pointed out earlier for enzyme reactions in general, low $\Delta G$'s between intermediate states will make such a cyclic reaction sequence kinetically optimal. Thus, the thermodynamic description of the photocycle of solubilized BR in this report contains nothing that would be contrary to transport function in the monomeric protein.

**Registry No.** Proton, 12408-02-5.

## REFERENCES


Albery, W. J., & Knowles, J. R. (1976) *Biochemistry 15*, 5631–5640.

Ames, J. B., & Mathies, R. A. (1990) *Biochemistry 29*, 7181–7190.

Baldwin, R. L. (1986) *Proc. Natl. Acad. Sci. U.S.A. 83*, 8069–8072.

Bamberg, E., Dencher, N. A., Fahr, A., & Heyn, M. P. (1981) *Proc. Natl. Acad. Sci. U.S.A. 78*, 7502–7506.

Bauer, P. J., Dencher, N. A., & Heyn, M. P. (1976) *Biophys. Struct. Mech. 2*, 79–92.

Becher, B., & Ebrey, T. G. (1976) *Biochem. Biophys. Res. Commun. 69*, 1–6.

Birge, R. R., Cooper, T. M., Lawrence, A. F., Masthay, M. B., Zhang, C. F., & Zidovetski, R. (1991) *J. Am. Chem. Soc.* (in press).

Blaurock, A. E., & Stoeckenius, W. (1971) *Nature 233*, 152–155.

Braiman, M. S., Mogi, T., Marti, T., Stern, L. J., Khorana, H. G., & Rothschild, K. J. (1988) *Biochemistry 27*, 8516–8520.

Brouillette, C. G., Muccio, D. D., & Finney, T. K. (1987) *Biochemistry 26*, 7431–7438.

Butt, H. J., Fendler, K., Bamberg, E., Tittor, J., & Oesterhelt, D. (1989) *EMBO J. 8*, 1657–1663.

Casadio, R., & Stoeckenius, W. (1980) *Biochemistry 19*, 3374–3381.

Casadio, R., Gutowitz, H., Mowery, P., Taylor, M., & Stoeckenius, W. (1980) *Biochim. Biophys. Acta 590*, 13–23.

Chernavskii, D. S., Chizhov, I. V., Lozier, R. H., Murina, T. M., Prokhorov, A. M., & Zubov, B. V. (1989) *Photochem. Photobiol. 49*, 649–653.

Cherry, R. J., Heyn, M. P., & Oesterhelt, D. (1977) *FEBS Lett. 78*, 25–30.

Czégé, J., Dér, A., Zimányi, L., & Keszthelyi, L. (1982) *Proc. Natl. Acad. Sci. U.S.A. 79*, 7273–7277.

Dencher, N. A., & Heyn, M. P. (1978) *FEBS Lett. 96*, 322–326.

Dencher, N. A., & Heyn, M. P. (1979) *FEBS Lett. 108*, 307–310.

Dencher, N. A., Kohl, K. D., & Heyn, M. P. (1983) *Biochemistry 22*, 1323–1334.

Fukuda, K., Ikegami, A., Nasuda-Kouyama, A., & Kouyama, T. (1990) *Biochemistry 29*, 1997–2002.

Gerwert, K., Hess, B., Soppa, J., & Oesterhelt, D. (1989) *Proc. Natl. Acad. Sci. U.S.A. 86*, 4943–4947.

Gerwert, K., Souvignier, G., & Hess, B. (1990) *Proc. Natl. Acad. Sci. U.S.A. 87*, 9774–9778.

Henderson, R., & Unwin, P. N. (1975) *Nature 257*, 28–32.

Henderson, R., Baldwin, J. M., Ceska, T. A., Zemlin, F., Beckmann, E., & Downing, K. H. (1990) *J. Mol. Biol. 213*, 899–929.

Heyn, M. P., Bauer, P.-J., & Dencher, N. A. (1975) *Biochem. Biophys. Res. Commun. 67*, 897–903.

Hofrichter, J., Henry, E. R., & Lozier, R. H. (1989) *Biophys. J. 56*, 693–706.

Koch, M. H. J., Dencher, N. A., Oesterhelt, D., Plöhn, H. J., Rapp, G., & Büldt, G. (1991) *EMBO J. 10*, 521–516.

Li, Q., Govindjee, R., & Ebrey, T. G. (1984) *Proc. Natl. Acad. Sci. U.S.A. 81*, 7079–7082.

Lozier, R. H., Niederberger, W., Ottolenghi, M., Sivorinovsky, G., & Stoeckenius, W. (1978) in *Energetics and Structure of Halophilic Microorganisms* (Caplan, S. R., & Ginzburg, M., Eds.) pp 123–139, Elsevier/North Holland, Amsterdam.

Milder, S. J., Thorgeirsson, T. E., Mierke, L. J. W., Stroud, R. M., & Kliger, D. S. (1991) *Biochemistry 30*, 1751–1761.

Murphy, K. P., Privalov, P., & Gill, S. J. (1990) *Science 52*, 559–561.

Oesterhelt, D., & Stoeckenius, W. (1974) *Methods Enzymol. 31*, 667–678.

Ormos, P. (1991) *Proc. Natl. Acad. Sci. U.S.A. 88*, 473–477.

Ort, D. R., & Parson, W. W. (1979) *Biophys. J. 25*, 355–364.

Otto, H., Marti, T., Holz, M., Mogi, T., Lindau, M., Khorana, H. G., & Heyn, M. P. (1989) *Proc. Natl. Acad. Sci. U.S.A. 86*, 9228–9232.

Sturtevant, J. (1977) *Proc. Natl. Acad. Sci. U.S.A. 74*, 2236–2240.
Tittor, J., Soell, C., Oesterhelt, D., Butt, H.-J., & Bamberg, E. (1989) *EMBO J. 8*, 3477–3482.
Vârô, G., & Lanyi, J. K. (1990) *Biochemistry 29*, 2241–2250.
Vârô, G., & Lanyi, J. K. (1991a) *Biochemistry 30*, 5008–5015.
Vârô, G., & Lanyi, J. K. (1991b) *Biochemistry 30*, 5016–5022.
Vârô, G., & Lanyi, J. K. (1991c) *Biophys. J. 59*, 313–322.
Vârô, G., Duschl, A., & Lanyi, J. K. (1990) *Biochemistry 29*, 3798–3804.
Walmsley, A. R., & Lowe, A. G. (1987) *Biochim. Biophys. Acta 901*, 2229–2238.
Zimányi, L., Keszthelyi, L., & Lanyi, J. K. (1989) *Biochemistry 28*, 5165–5172.

# Effects of Melittin on Molecular Dynamics and Ca-ATPase Activity in Sarcoplasmic Reticulum Membranes: Electron Paramagnetic Resonance†

James E. Mahaney and David D. Thomas*
*Department of Biochemistry, University of Minnesota Medical School, Minneapolis, Minnesota 55455*
*Received February 11, 1991; Revised Manuscript Received May 10, 1991*

ABSTRACT: We have performed electron paramagnetic resonance (EPR) experiments on nitroxide spin labels incorporated into rabbit skeletal sarcoplasmic reticulum (SR), in order to investigate the physical and functional interactions between melittin, a small basic membrane-binding peptide, and the Ca-ATPase of SR. Melittin binding to SR substantially inhibits $Ca^{2+}$-dependent ATPase activity at 25 °C, with half-maximal inhibition at 9 mol of melittin bound per mole of Ca-ATPase. Saturation transfer EPR (ST-EPR) of maleimide spin-labeled Ca-ATPase showed that melittin decreases the submillisecond rotational mobility of the enzyme, with a 4-fold increase in the effective rotational correlation time ($\tau_r$) at a melittin/Ca-ATPase mole ratio of 10:1. This decreased rotational motion is consistent with melittin-induced aggregation of the Ca-ATPase. Conventional EPR was used to measure the submicrosecond rotational dynamics of spin-labeled stearic acid probes incorporated into SR. Melittin binding to SR at a melittin/Ca-ATPase mole ratio of 10:1 decreases lipid hydrocarbon chain mobility (fluidity) 25% near the surface of the membrane, but only 5% near the center of the bilayer. This gradient effect of melittin on SR fluidity suggests that melittin interacts primarily with the membrane surface. For all of these melittin effects (on enzymatic activity, protein mobility, and fluidity), increasing the ionic strength lessened the effect of melittin but did not alleviate it entirely. This is consistent with a melittin–SR interaction characterized by both hydrophobic and electrostatic forces. Since the effect of melittin on lipid fluidity alone is too small to account for the large inhibition of Ca-ATPase rotational mobility and enzymatic activity, we propose that melittin inhibits the ATPase primarily through its capacity to aggregate the enzyme, consistent with previous observations of decreased Ca-ATPase activity under conditions that decrease protein rotational mobility.

Understanding the relationship between molecular dynamics and enzymatic activity within a biological membrane is a vital step toward constructing an accurate model describing the overall functioning of the membrane system. Concerning skeletal muscle sarcoplasmic reticulum (SR)[1] membranes, intensive research effort has been devoted to such an understanding; that is, to understand precisely how the molecular motions and interactions of both the Ca-ATPase, the major integral membrane protein of SR, and the lipids within the SR membrane contribute to the optimal functioning of calcium uptake.

Since the rotational mobility (diffusion coefficient) of an integral membrane protein about the membrane normal depends inversely on both the protein's cross-sectional area and the lipid hydrocarbon chain viscosity (Saffman & Delbrück, 1975), a variety of mechanisms designed to alter the physical state of the protein and the bilayer have been employed in order to correlate these perturbations with resultant Ca-ATPase functioning. Inducing lateral aggregation of the enzyme by either (a) changing temperature (Bigelow et al., 1986; Squier et al., 1988b; Birmachu & Thomas, 1990), (b) selectively cross-linking the Ca-ATPase (Squier et al., 1988a), (c) decreasing the lipid/protein ratio (Squier & Thomas, 1988), or (d) crystallizing the ATPase by using vanadate (Lewis & Thomas, 1986) has a profound inhibitory effect on both ATP hydrolysis and calcium uptake by SR. Increasing the fluidity (decreasing the viscosity) of the SR lipids adjacent to the protein results in an increased rate of Ca-ATPase rotation and a concomitant increase in Ca-ATPase activity (Bigelow & Thomas, 1987). The results of these studies indicate that optimal Ca-ATPase enzymatic function correlates directly with the ability of the Ca-ATPase to undergo microsecond rotational motion in a fluid lipid bilayer. Similar studies of other membrane-enzyme systems show that changes in lipid chain unsaturation or levels of cholesterol (which alter the fluidity of the bilayer) can have profound effects on function (Benga

† This work was supported by NIH Grant GM27906 to D.D.T. J.E.M. was supported by a postdoctoral fellowship from the American Heart Association.
* Author to whom correspondence should be addressed.

[1] Abbreviations: SR, sarcoplasmic reticulum; NEM, *N*-ethylmaleimide; MSL, maleimide spin label; SASL, stearic acid spin label; PCSL, phosphatidylcholine spin label; MOPS, 3-(*N*-morpholino)propanesulfonic acid; ATP, adenosine triphosphate; EPR, electron spin resonance; ST-EPR, saturation transfer EPR; $\int V_2'$, ST-EPR integrated intensity parameter; TPX, tetramethylene polymer plastic.

0006-2960/91/0430-7171$02.50/0 